Electronic Supplementary Material (ESI) for Analyst.

Supplementary Figures 1-12, Supplementary Tables 1, and Supplementary Materials and Methods

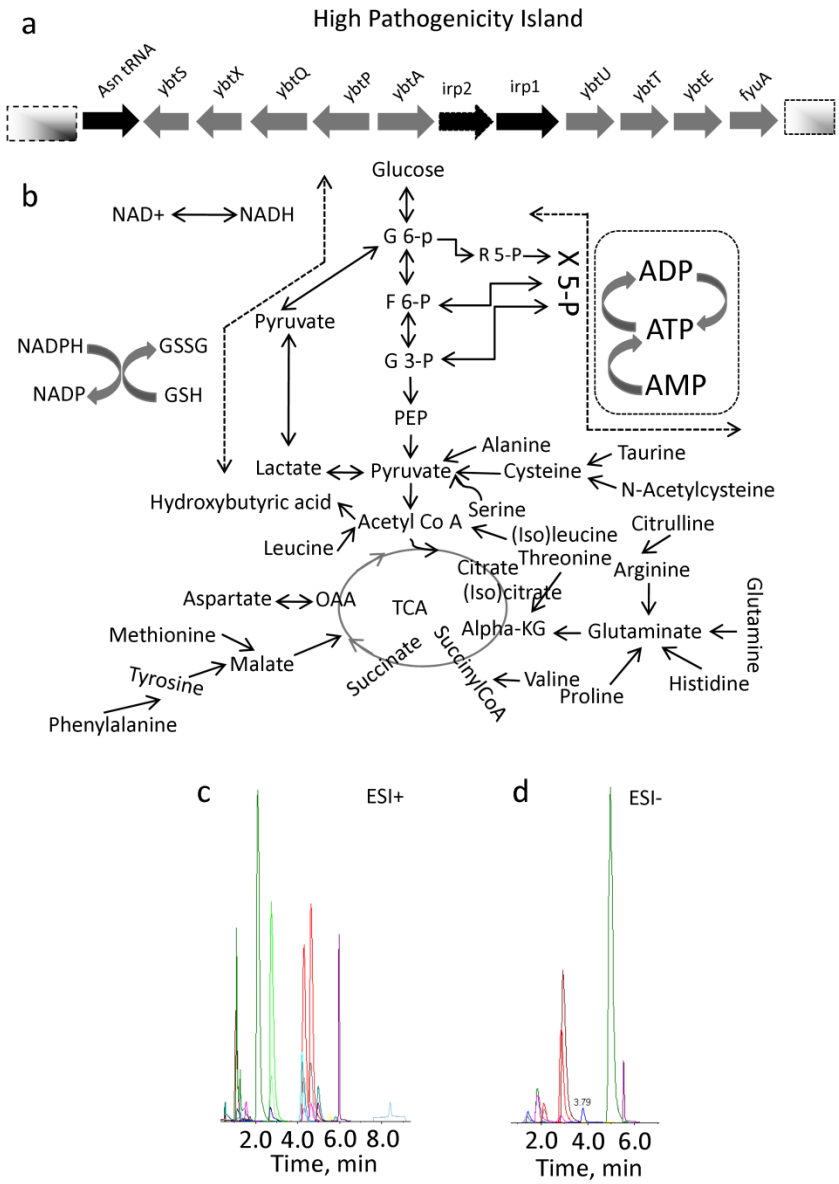

Supplementary Figure 1 Schematic illustration for how LC-MS-based metabolomic profiling helps to define the genotypic traits of the high-pathogenicity island (HPI) in UPEC. (a) Genomic structure of the HPI. (b) Core metabolic pathways incorporated into CCM. (c) (d) LC-MS analysis of hydrophilic metabolites involved in CCM by positive (ESI+) and negative (ESI-) multiple monitoring reaction modes.

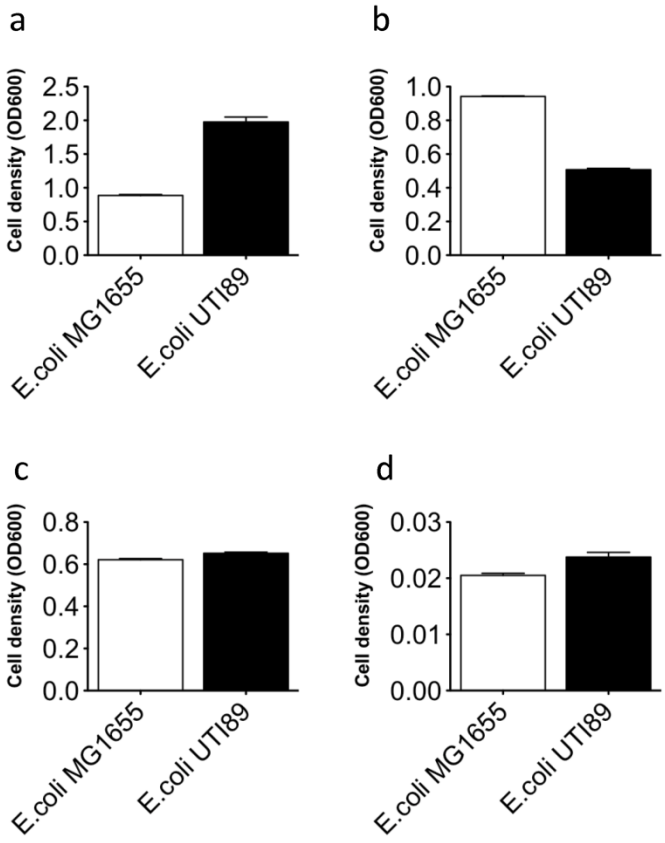

Supplementary Figure 2 Bacterial cell densities (OD600/mL) of UPEC and non-UPEC cultures after 18 hours of incubation in (a) LB broth, (b) M63 minimal medium (0.2% glycerol), (c) M63 minimal medium (without 0.2% glycerol and with 0.2% glucose) and (d) M63 minimal medium (without 0.2% glycerol).

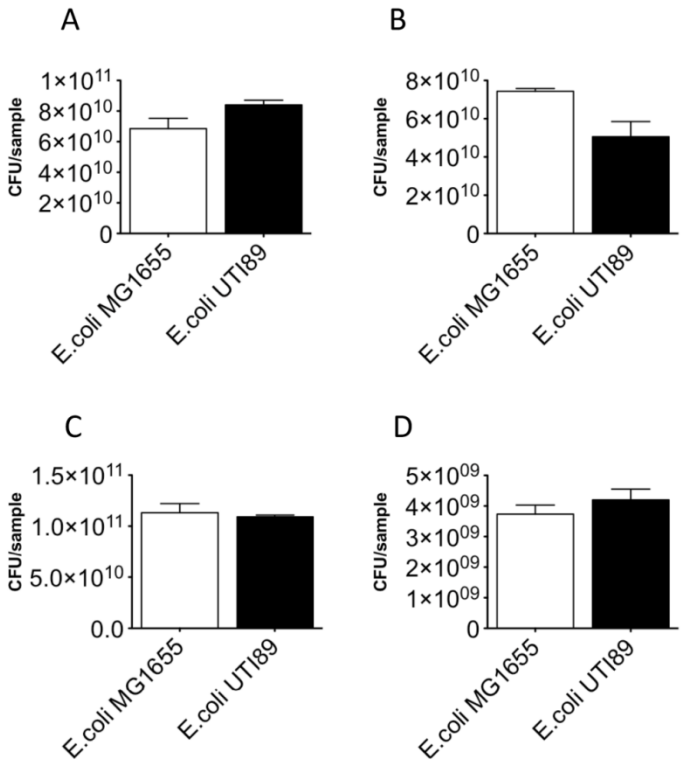

Supplementary Figure 3 Bacterial cell density (CFU/sample) of UPEC and non-UPEC cultures after eighteen hours of incubation in (a) LB broth, (b) M63 minimal medium (0.2% glycerol), (c) M63 minimal medium (without 0.2% glycerol and with 0.2% glucose) and (d) M63 minimal medium (without 0.2% glycerol). The CFUs were calculated by serial dilution and overnight incubation on LB agar plates.

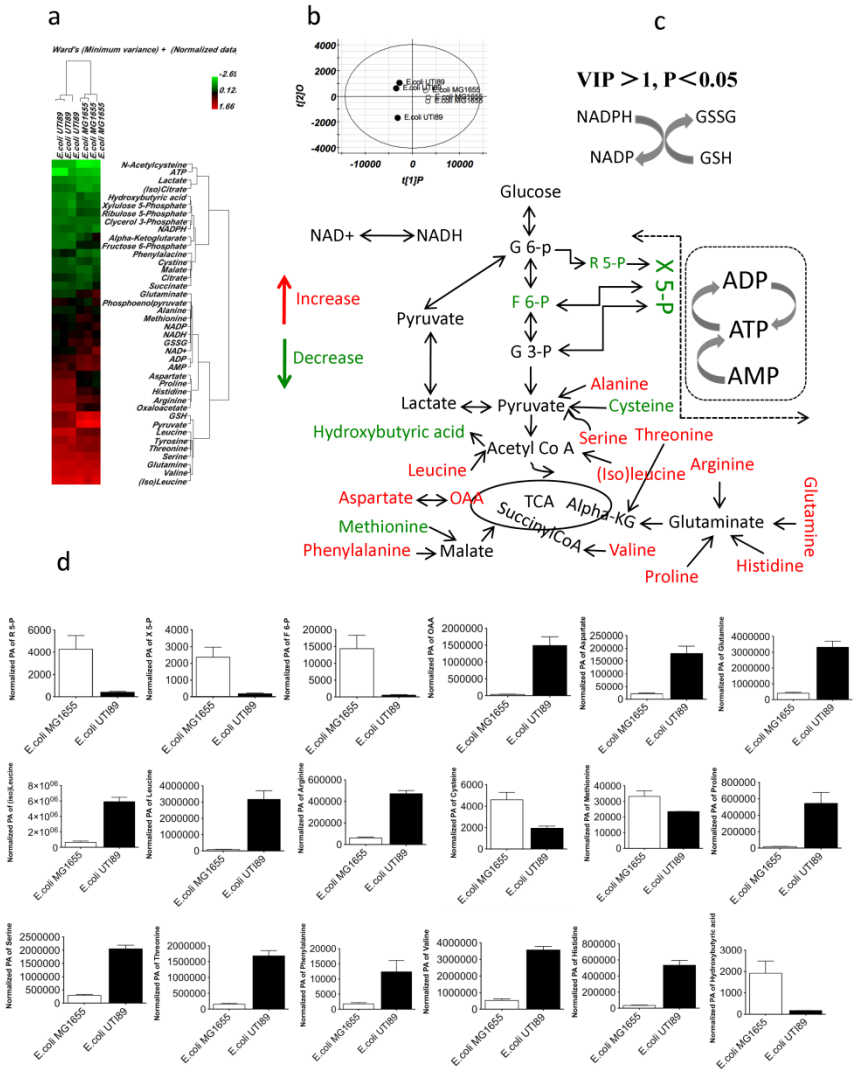

Supplementary Figure 4 Central carbon metabolism in UPEC UTI89 (+HPI) and non-UPEC MG1655 (-HPI) incubated in LB broth. (a) Unsupervised heatmap of relative levels of hydrophilic metabolites involved in CCM clustered by hierarchical clustering analysis (HCA) (Supplementary Methods online). (b) Supervised OPLS-DA scatter plot of relative levels of hydrophilic metabolites involved in CCM; R2Y: 0.9, Q2:0.95. (c) The metabolites whose changed levels distinguish UTI89 from MG1655 are highlighted and color coded within a background of relevant metabolic pathways with a cutoff of VIP > 1, < 0.05. Metabolites that were more abundant in UTI89 than in MG1655 are highlighted in red, while green shows metabolites present at a lower level in UTI89 than in MG1655. (d) Histograms showing the expression levels of the metabolites that are differentially expressed in MG1655 and UTI89.

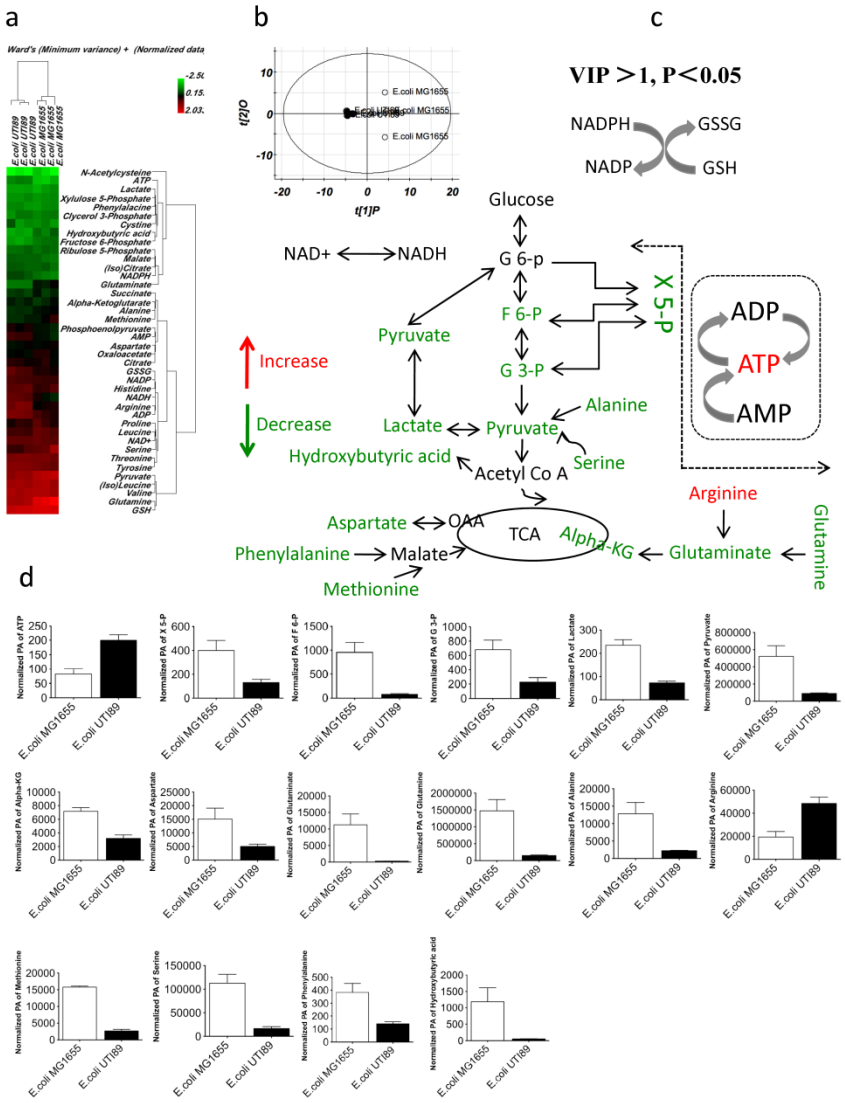

Supplementary Figure 5 Central carbon metabolism in UPEC UTI89 (+HPI) and non-UPEC MG1655 (-HPI) when incubated in M63 minimal medium. (a) Unsupervised heatmap of the relative levels of CCM-involved hydrophilic metabolites clustered by hierarchical clustering analysis (HCA) (Supplementary Methods online). (b) Supervised OPLS-DA scatter plot of the relative levels of hydrophilic metabolites involved in CCM; R2Y: 0.86, Q2:0.92. (c) The metabolites whose changed levels distinguish UTI89 from MG1655 are highlighted and color coded for the relevant metabolic pathways with a cutoff of VIP > 1, P < 0.05. Metabolites that were more abundant in UTI89 than in MG1655 are highlighted in red, whereas green shows metabolites present at a lower level in UTI89 than in MG1655. (d) Histograms showing the expression levels of selected metabolites in MG1655 and UTI89.

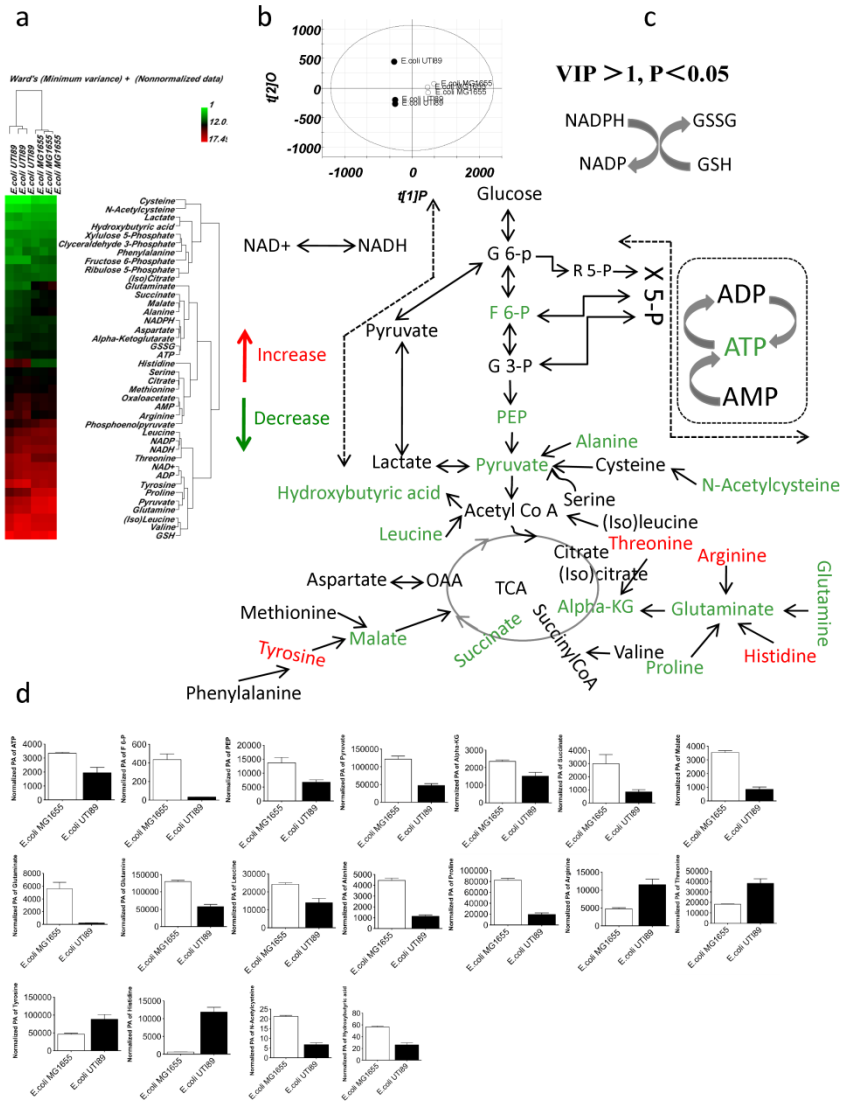

Supplementary Figure 6 Central carbon metabolism in UPEC UTI89 (+HPI) and non-UPEC MG1655 (-HPI) when incubated in M63 minimal medium (-0.2% glycerol + 0.2 glucose). (a) Unsupervised heatmap of the relative levels of hydrophilic metabolites involved in CCM clustered by hierarchical clustering analysis (HCA) (Supplementary Methods online). (b) Supervised OPLS-DA scatter plot of the relative levels of hydrophilic metabolites involved in CCM; R2Y: 0.88, Q2:0.94. (c) The metabolites whose changed levels distinguish UTI89 from MG1655 are highlighted and color coded for the relevant metabolic pathways with a cutoff of VIP > 1, P < 0.05. Metabolites that were more abundant in UTI89 than in MG1655 are highlighted in red, whereas green shows metabolites present at a lower level in UTI89 than in MG1655. (d) Histograms showing the expression levels of selected metabolites in MG1655 and UTI89.

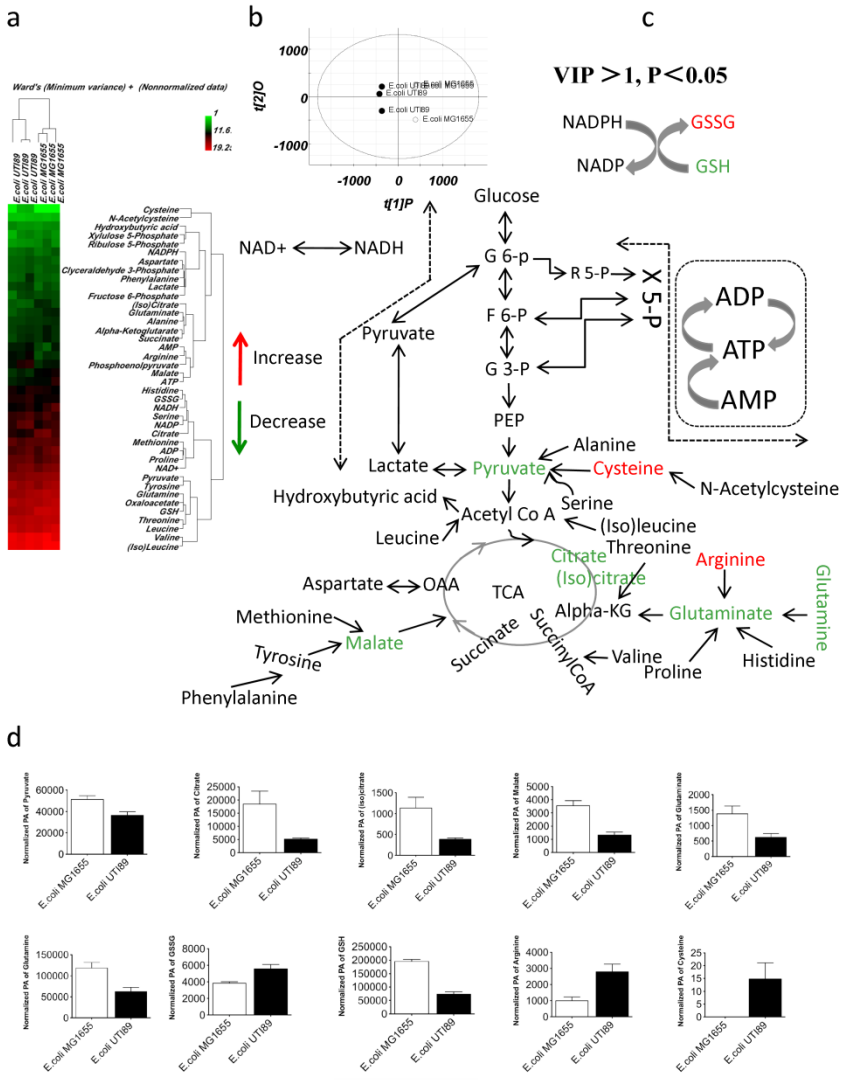

Supplementary Figure 7 Central carbon metabolism in UPEC UTI89 (+HPI) compared to non-UPEC MG1655 (-HPI) when incubated in M63 minimal medium (-0.2% glycerol). (a) Unsupervised heatmap of the relative levels of CCM-involved hydrophilic metabolites clustered by hierarchical clustering analysis (HCA) (Supplementary Methods online). (b) Supervised OPLS-DA scatter plot of the relative levels of hydrophilic metabolites involved in CCM; R2Y: 0.87, Q2:0.96. (c) The metabolites whose changed levels distinguish UTI89 from MG1655 are highlighted and color coded for the relevant metabolic pathways with a cutoff of VIP > 1, P < 0.05. Metabolites that were more abundant in UTI89 than in MG1655 are highlighted in red, whereas green shows metabolites present at a lower level in UTI89 than in MG1655. (d) Histograms showing the expression levels of selected metabolites in MG1655 and UTI89.

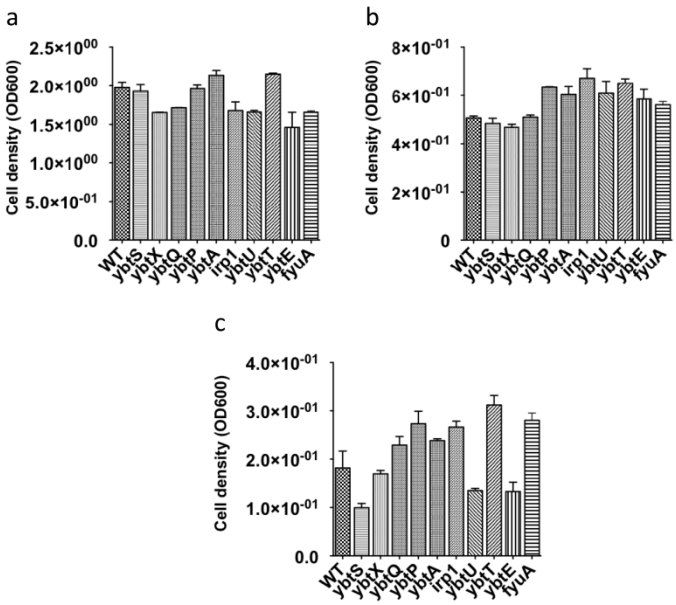

Supplementary Figure 8 Bacterial cell density (OD600) of wild-type UPEC (UTI89) and UTI89 mutants after eighteen hours of culture in (a) LB broth, (b) M63 minimal medium, and (c) pooled fresh urine. The CFUs were calculated after serial dilution and overnight incubation on LB agar plates.

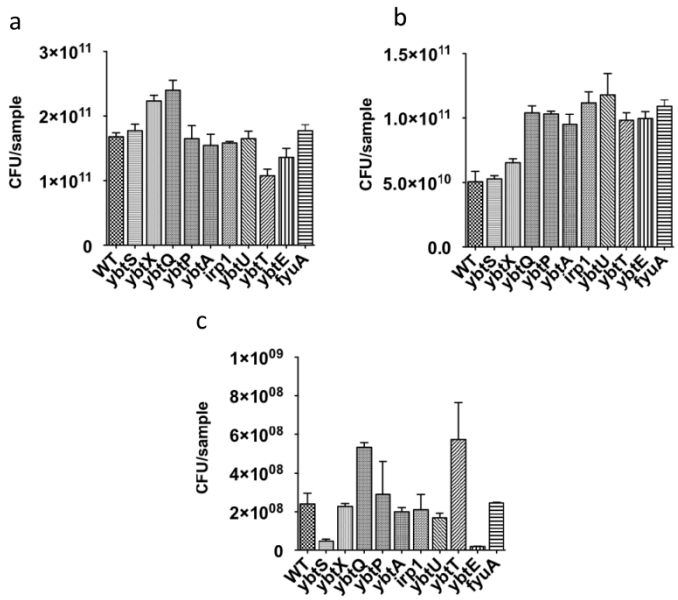

Supplementary Figure 9 Bacterial cell density (CFU/sample) of wild-type UPEC (UTI89) and UTI89 mutants after eighteen hours of culture in (a) LB broth, (b) M63 minimal medium, and (c) pooled fresh urine. The CFUs were calculated after serial dilution and overnight incubation on LB agar plates.

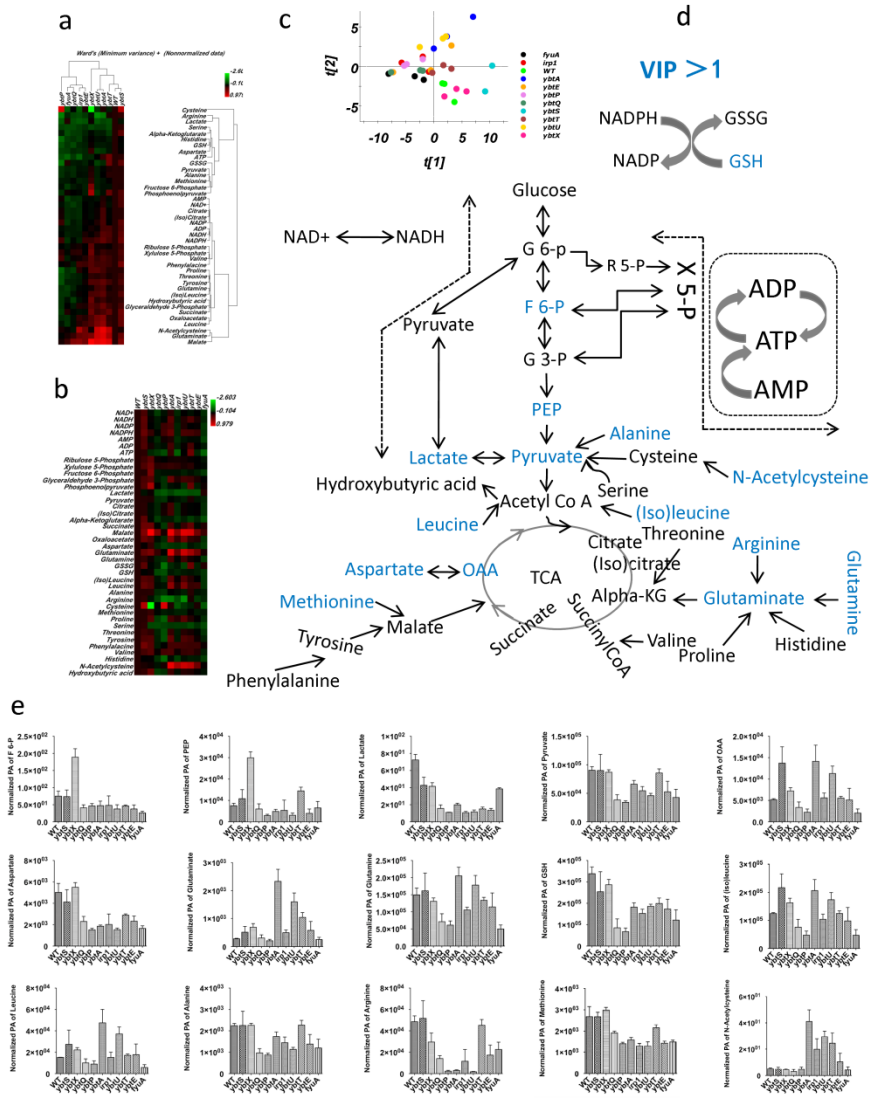

Supplementary Figure 10 HPI virulence genes influence the CCM of UPEC (UTI89) when cultured in M63 minimal medium. (a)(b) Unsupervised heatmap of the relative levels of the hydrophilic metabolites involved in CCM clustered by hierarchical clustering analysis (HCA) and sequenced by metabolic pathway (Supplementary Methods online). (c) Supervised OPLS-DA scatter plot of the relative levels of hydrophilic metabolites involved in CCM; R2Y: 0.82, Q2:0.90. (d) The metabolites whose changed levels distinguish wild-type UTI89 from the mutants are highlighted and colored blue for the relevant metabolic pathways with a cutoff of VIP > 1. (e) Histograms showing the expression levels of selected metabolites for the various strains.

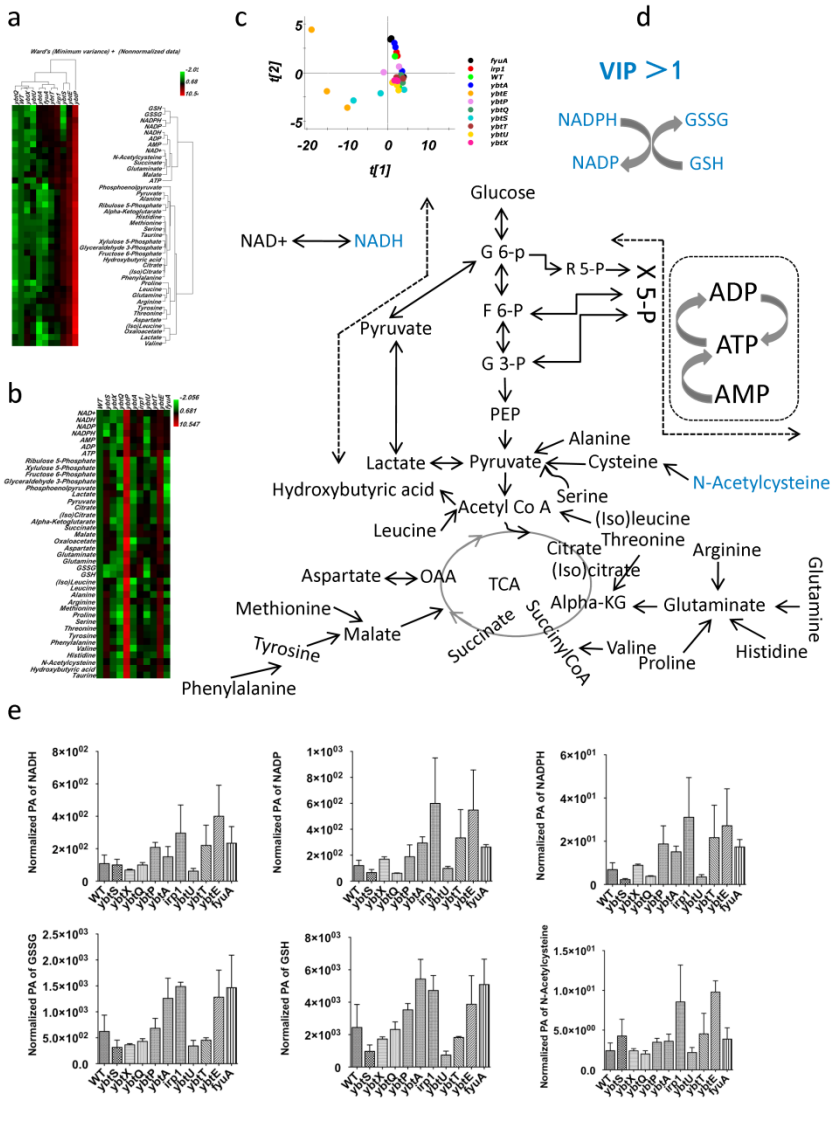

Supplementary Figure 11 The influence of HPI genes on CCM in UPEC (UTI89) when cultured in pooled fresh urine. (a)(b) Unsupervised heatmap of the relative levels of hydrophilic metabolites involved in CCM clustered by hierarchical clustering analysis (HCA) and sequenced by metabolic pathway (Supplementary Methods online). (c) Supervised OPLS-DA scatter plot of the relative levels of hydrophilic metabolites involved in CCM; R2Y: 0.83, Q2:0.88. (d) The metabolites whose changed levels distinguish wild-type UTI89 from the mutants are highlighted and colored blue for the relevant metabolic pathways with a cutoff of VIP > 1. (e) Histograms showing the expression levels of selected metabolites for the various strains.

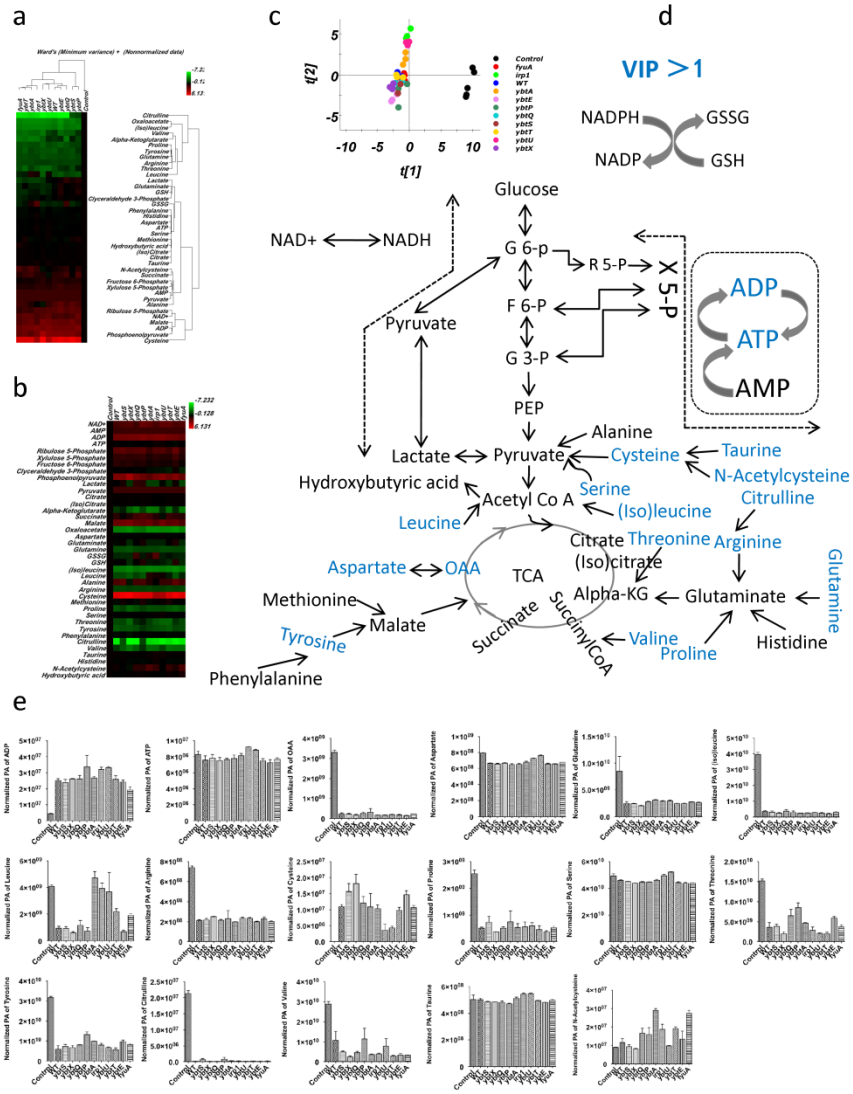

Supplementary Figure 12 Differences in the levels of metabolites involved in CCM between pooled fresh urine and conditioned culture supernatant after incubation of wild-type UTI89 or UTI89 mutants. (a)(b) Unsupervised heatmap of the relative levels of CCM-involved hydrophilic metabolites clustered by hierarchical clustering analysis (HCA) and sequenced by metabolic pathway (Supplementary Methods online). (c) Supervised OPLS-DA scatter plot of the relative levels of hydrophilic metabolites involved in CCM; R2Y: 0.81, Q2:0.94. (d) The metabolites whose changed levels distinguish wild-type UTI89 from the mutants when compared to fresh urine are highlighted and colored blue for the relevant metabolic pathways with a cutoff of VIP > 1. (e) Histograms showing the expression levels of selected metabolites among the strains.

Supplementary Table 1 Multiple reaction monitoring (MRM) parameters of the LC-MS method for analyzing hydrophilic metabolites involved in central carbon metabolism

Metabolite ID	Q1 mass (Da)	Q3 mass (Da)	Time (min)	Dp (volts)	Ep (volts)	CE (volts)	CXP (volts)	Ion mode
NAD+	662.156	540	5	-60	-10	-20	-17	ESI-
NADH	665	136	5.1	86	10	42	10	ESI+
NADP	742.146	620.1	2.9	-65	-10	-24	-17	ESI-
NADPH	746	136	3.1	81	10	62	20	ESI+
AMP	348.065	136.1	2.7	266	10	29	10	ESI+
ADP	426.088	79	1.9	-65	-10	-78	-1	ESI-
ATP	506.035	158.7	2	-60	-10	-36	-11	ESI-
Ribulose 5-Phosphate	229.1	79.1	1.3	-60	-10	-46	-3	ESI-
Xylulose 5-Phosphate	228.9	97	1.3	-45	-10	-16	-5	ESI-
Fructose 6-Phosphate	258.9	96.8	1.3	-60	-10	-20	-5	ESI-
Glyceraldehyde 3-Phosphate	170.9	79	1.3	-45	-10	-22	-1	ESI-
Phosphoenolpyruvate	166.8	78.7	1.5	-35	-10	-13	-7	ESI-
Lactate	89	43	2.4	-40	-10	-18	-5	ESI-
Pyruvate	89.1	72.2	1	46	10	19	4	ESI+
Citrate	191.1	111	2.9	-30	-10	-22	-15	ESI-
(Iso)Citrate	191.1	173	2.9	-30	-10	-16	-17	ESI-
Alpha-Ketoglutarate	144.9	101.1	2.1	-30	-10	-12	-5	ESI-
Succinate	117.1	73	3.9	-25	-10	-14	-1	ESI-
Malate	133.2	115	1.8	-30	-10	-15	-5	ESI-
Oxaloacetate	132.1	86.1	4.8	86	10	15	6	ESI+
Aspartate	133.2	87.1	1.6	31	10	15	6	ESI+
Glutamate	145.9	127.9	1.3	-45	-10	-16	-7	ESI-
Glutamine	147.1	84.1	1.3	41	10	25	14	ESI+
GSSG	611.2	306.2	5.5	-90	-10	-34	-13	ESI-
GSH	308.1	76.1	2.7	66	10	39	4	ESI+
(Iso)Leucine	132.1	86	4.8	36	10	15	14	ESI+
Leucine	132.1	86.1	4.3	71	10	15	6	ESI+
Alanine	90.3	73	1	56	10	19	6	ESI+
Arginine	175.1	70.1	1.2	61	10	33	4	ESI+
Cysteine	240.9	152	3.6	66	10	19	12	ESI+
Methionine	149.2	59.1	8.4	26	10	17	10	ESI+
Proline	116.1	70.2	1.5	51	10	21	4	ESI+
Serine	105.1	64	1.1	11	10	7	4	ESI+
Threonine	120.1	103	5.9	91	10	25	6	ESI+
Tyrosine	182.1	136.1	4.2	46	10	19	10	ESI+
Phenylalanine	166.1	120	7.4	31	10	19	26	ESI+
Valine	118.2	72	2.1	26	10	15	12	ESI+
Histidine	156.1	110	1.2	36	10	21	6	ESI+
N-Acetylcysteine	161.9	83.9	5.6	-45	-10	-12	-5	ESI-
Hydroxybutyric acid	102.9	59	4.3	-45	-10	-14	-1	ESI-
Citrulline	173.9	131	1.4	-50	-10	-16	-9	ESI-
Taurine	126.1	108	1.3	66	10	17	8	ESI+
Ferric-yersiniabactin	535.6	188.5	6.9	110	10	35	12	ESI+
^{13}C-Ferric-yersiniabactin	556.6	196.5	6.9	110	10	35	12	ESI+

Supplementary Materials and Methods

Chemicals and reagents

Acetonitrile (HPLC grade), formic acid (LC/MS grade) and water (LC/MS grade) were purchased from Fisher Scientific (Fisher Scientific, Pittsburg, PA, USA); the standard compounds of NAD+, NADH, NADP, NADPH, AMP, ADP, ATP, ribulose 5-phosphate (R 5-P), xylulose 5-phosphate (X 5-P), fructose 6-phosphate (F 6-P), glyceraldehyde 3-phosphate (G 3-P), phosphoenolpyruvate (PEP), lactate, pyruvate, citrate, (iso)citrate, alpha-ketoglutarate (Alpha-KG), succinate, malate, oxaloacetate (OAA), aspartate, glutaminate, glutamine, reduced glutathione (GSH), oxidized glutathione (GSSG), (iso)leucine, leucine, alanine, arginine, cysteine, methionine, proline, serine, threonine, tyrosine, phenylalanine, valine, histidine, N-acetylcysteine, hydroxybutyric acid, taurine, and citrulline were purchased from Sigma (Sigma-Aldrich Corp., Saint Louis, MO, USA). All other used reagents were all ACS grade reagents.

Ultra-Fast Liquid Chromatography-Mass Spectrometry (LC-MS)

According to previous publication (1, 2), and somewhat modifications have been made relative to our current LC-MS platform. Ultra-fast liquid chromatography (UFLC) (Shimadzu, Kyoto, Japan) consisted of two LC-20AD XR pumps, a DGU-20A3 prominence vacuum degasser, an SIL-20AXR autosampler, a CTO-20A prominence column oven, and a CBM-20A communications bus module, coupled with a hybrid API 4000 QTrap and API 3200 TQ (AB Sciex, Foster City, CA, USA) with an Turbo V ESI ionization source interface, and a computer platform equipped with a Solution Analyst software version 1.5.2 (AB Sciex, Foster City, CA, USA) was used for data acquisition and pre-processing.

Targeted Metabolomics analysis of hydrophilic metabolites was performed on a Acquity HSS T3 column (150 mm × 2.0 mm, 1.7 µm, waters) using a gradient: 0-27% B over 8 min, then B increase to 99% from 8 to 10 min (A: 0.1% formic acid in water; B: 0.1% formic acid in acetonitrile) at a flow rate of 0.3 mL/min. The samples were analyzed by UFLC/MS system in positive or negative ionization modes with an electrospray ionization voltage of 5500 V for positive mode and -4500 V for negative mode, nebulizer gas (air) and turbo gas (air) settings at 50 and 50 psi, and a turbosource gun temperature of 500°C. The curtain gas (nitrogen) was set at

25 psi, the collision cell pressure at low or high mode for different purposes. The MRM parameter for each metabolite is recorded in **Supplementary Table 1**.

LC-MS determination of yersiniabactin was performed on a Betasil C18 Column (50 mm × 2.1 mm, 5.0 μm, Thermo Scientific) with a gradient as follows: 2.0-65 % B over 10 min (A: 0.1% formic acid in water; B: 0.1% formic acid in acetonitrile) at a flow rate of 0.4 mL/min. The MRM parameter is listed in **Supplementary Table 1**.

Sample preparation

Extraction of hydrophilic metabolites (2)

Firstly, cell pellets were isolated from 50 mL of culture solution, fast quenched with ice-cold methanol by spinning down to 11,500 × g at 4 °C for 10 min, mixed with 1.2 mL of 80% ice-cold methanol by vortexing for 30 s, and kept on dry ice for 30 min.. Secondly, 30 dunces of homogenization was done to the sample and spun down to 23008×g at 4 °C for 10 min, the supernatant was collected to completely mix with 800 μl of acetonitrile kept on ice for 15 minutes. Thirdly, the supernatant was isolated to lyophilized for sixteen hours. All above procedure should be performed within safety hood. Finally, the dried sample was re-dissolved with 1 ml of distill water, and 5 μl of solution was analyzed by LC-MS.

Preparation of ^{13}C-labeled internal standards

To see our previous publication (4)

Extraction of siderophore yersiniabactin (2)

6 μL of 0.1 M ferric chloride and 50 μL of ^{13}C-labeled internal standard were added to 1 mL of cell supernatant to a final concentration of 0.1 mM. After 15 minute room temperature incubation, the precipitate was removed by centrifugation. The supernatant was applied to a 96-well cartridge filled with C18 micro-column pre-conditioned with 0.5 mL of methanol and 0.5 mL of distill water wash continually. The loaded column was washed with 0.5 mL of 20% methanol, and siderophore yersiniabactin was eluted with 0.5 mL of 80% methanol. 10 μl of elute was injected into LC-MS for analysis.

Bacterial strains and cultivation

To examine siderophore yersiniabactin production in liquid culture and CCM associated hydrophilic metabolites in bacteria cell pellet, our protocol has been established by referring to the previous publication (3, 4), but some modifications have been made. Briefly, 4 hour cultures of *E. coli* grown in LB broth medium were diluted 1:100 into diverse conditioned medium and incubated for 18 h at 37 °C in a rotary shaker.

The composition of conditioned culture medium

1) LB broth medium

2) M63 minimal medium containing 0.2% glycerol and 10 mg/mL niacin

3) M63 minimal medium containing 0.2% glucose and 10 mg/mL niacin

4) Fresh pooled urine was prepared by equal volume of mixing 8 volunteers of health, and filtered with 0.22 μl of filter for removing any contaminants before incubation.

Deletion strain construction

Deletion mutations were made using the red recombinase method, as previously described, using pKD4 or pKD13 as a template (4-6). PCR was performed with flanking primers to confirm the appropriate deletions. Antibiotic insertions were removed by transforming the mutant strains with pCP20 (7) expressing the FLP recombinase. The resultant strains subsequently had no additional antibiotic resistance compared with the parental wt strain.

Chemometric Analysis

Chemometric analyses were performed using SIMCA-P+ version 12.0.1 (Umetrics) with supervised orthogonal partial least square discriminate analysis (OPLS-DA). Variables were firstly normalized to CFU value and factors of volume, then were scaled to a Pareto distribution to ensure equal contributions from each variable to the models. To provide an overview of the data we used FDA Genomic Tool (ArrayTrack™) (8) to plot a heatmap with log 2 transformation of normalized, median-centered data prior to clustering with ward and auto-scale.

Statistical analysis

Statistics and graphs were generated using GraphPad Prism 5. Statistical differences in metabolite expression between groups were calculated using one-way ANOVA and Tukey's test. Statistical differences are considered significant when the test p value is less than 0.05 (*) and 0.01 (**).

REFERENCES

1. Lv, H. *et al*. *J. Proteome Res.* **10**, 2104-2012 (2011).
2. Lv, H. et al. *J Proteome Res.* **13,** 1397-1404 (2014).
3. Valdebenito, M. *et al. Int. J. Med. Microbiol.* **295**, 99–107 (2005).
4. Henderson, J. P. *et al. PLoS Pathog.* **5**, e1000305 (2009).
5. Datsenko, K. A. *et al. Proc Natl Acad Sci U S A* 97, 6640–6645 (2000).
6. Murphy, K.C. *et al. BMC Mol. Biol.* 4, 11 (2003).
7. Cherepanov, P. P. *et al. Gene* 158,9–14 (1995).
8. Tong, W. *et al. EHP Toxicogenomics* 111, 1819-1826 (2003).